Materials Horizons

ROYAL SOCIETY OF CHEMISTRY

FOCUS

View Article Online
View Journal

Cite this: DOI: 10.1039/d6mh00129g

Harnessing the energy gap law for high NIR-II quantum yield at the molecular and aggregate levels

Yi Qin,[a] Dong Wang *[a] and Ben Zhong Tang *[b]

Received 23rd January 2026,
Accepted 13th May 2026

DOI: 10.1039/d6mh00129g

rsc.li/materials-horizons

Fluorescence imaging in the second near-infrared window (NIR-II, 1000–1700 nm) has emerged as a powerful modality in biomedical research over the past decade, attracting broad scientific interest. Among various NIR-II emissive materials, small organic molecules have garnered particular attention due to their well-defined chemical structures, tunable photophysical properties and good biocompatibility. Despite notable progress in this field, most reported NIR-II fluorophores still suffer from low quantum yields (QYs), a fundamental limitation governed by the energy gap law, which significantly restricts their performance in advanced bioimaging applications. Overcoming the constraints imposed by this law on NIR-II QYs thus remains a critical and unresolved challenge. In this Focus Article, we first elucidate the photophysical origin of low QYs observed in NIR-II small molecules. We then systematically outline recent strategies aimed at enhancing their emission efficiency, both at the molecular and aggregate levels. Finally, we provide a forward-looking perspective on promising research directions, with the aim of stimulating further innovation and effort in this rapidly evolving frontier.

1. Introduction

Fluorescence imaging (FLI) technology has exhibited significant value in biomedical and basic research due to its high sensitivity, capacity for real-time feedback, broad applicability, and cost-effectiveness.[1–4] In comparison to imaging in the visible or first near-infrared (NIR-I) window, fluorescence imaging conducted in the second near-infrared (NIR-II, 1000–1700 nm) region offers several distinct advantages: (1) a higher signal-to-background ratio, attributable to reduced tissue

[a] Center for AIE Research, Shenzhen Key Laboratory of Polymer Science and Technology, College of Materials Science and Engineering, Shenzhen University, Shenzhen 518060, China. E-mail: wangd@szu.edu.cn
[b] School of Science and Engineering, Guangdong Basic Research Center of Excellence for Aggregate Science, Shenzhen Institute of Aggregate Science and Technology, The Chinese University of Hong Kong, Shenzhen (CUHK-Shenzhen), Guangdong 518172, China. E-mail: tangbenz@cuhk.edu.cn

Yi Qin

Yi Qin received his PhD degree in chemistry from East China Normal University in 2020. Then he conducted his postdoctoral study at Shenzhen University. He is currently an assistant professor at Shenzhen University. His research focuses on the design of NIR-II AIE materials for biological applications.

Dong Wang

Dong Wang received his PhD degree from Bordeaux University and conducted his postdoctoral study at University of Toronto and HKUST. He is currently a distinguished professor at Shenzhen University. His research focuses on the design of AIEgens for biological applications.

autofluorescence; (2) greater tissue penetration depth, resulting from lower scattering and absorption of biological tissues within the NIR-II region; and (3) minimal photodamage to healthy tissues on account of the lower energy of long-wavelength light.[5,6] Furthermore, the relatively small energy gap between the ground and excited states in NIR-II fluorophores promotes non-radiative decay pathways, thereby enabling concurrent applications in photoacoustic/photothermal imaging through localized heat generation.[7,8] Capitalizing on these advantages, NIR-II fluorescence imaging has recently received enormous research interest and a variety of luminescent materials in the NIR-II window, including inorganic nano-materials and organic molecules, have been prepared and exhibit widespread applications in theranostics of cancer, infectious diseases, cardiovascular and cerebrovascular diseases and so on.[9–11]

Among diverse NIR-II emissive materials, small organic fluorophores operating within this window have garnered considerable scientific interest owing to their well-defined chemical structures, tunable photophysical properties, favorable biocompatibility, low systemic toxicity and straightforward structural modification.[12–14] Pioneering work in this field was reported by Dai *et al.* in 2016,[15] who demonstrated that a 970-Da organic molecule CH1055 performed better than the FDA approved dye ICG in lymphatic imaging, orthotopic glioblastoma brain tumor imaging and image-guided tumor surgery. Subsequently, a variety of structurally distinct NIR-II small molecules, including "donor–acceptor–donor (D–A–D)" adducts, cyanine-type dyes, BODIPY/rhodamine derivatives and xanthonoid derivatives, have been synthesized and applied in phototheranostics.[16–20] For instance, Wang *et al.* developed a "D–A–D" type NIR-II molecule, DPBTA-DPTQ, with maximum absorption/emission wavelengths at 806/1120 nm, which exhibited excellent efficacy in multimodal imaging-guided tumor ablation.[21] Additionally, Cheng and colleagues constructed a quinoxaline-based NIR-II molecule FT-TQT, which combined high fluorescence quantum yield with good chemical stability and enabled real-time monitoring of tumor-associated angiogenesis in murine models.[22]

It should be noted that, despite extensive research on NIR-II small molecules, the fluorescence quantum yields (QYs) of currently reported molecules remain notably low (usually less than 1%), and particularly below 0.01% in the region beyond 1200 nm. According to the energy gap law,[23–25] QYs generally decline as emission wavelength increases, presenting a significant challenge for achieving high brightness in the NIR-II window. Consequently, devising strategies to mitigate the influence of the energy gap law on quantum efficiency represents a critical yet unresolved issue in this field. Herein, we will start with the origin of low QYs of NIR-II small molecules, followed by a systematic discussion of potential design strategies and future research directions aimed at enhancing their luminescent performance.

Ben Zhong Tang

Ben Zhong Tang received his BS and PhD degrees from South China University of Technology and Kyoto University in 1982 and 1988, respectively. He conducted postdoctoral research at University of Toronto from 1989 to 1994. He joined the Hong Kong University of Science and Technology in 1994 and was promoted to Chair Professor in 2008. He was elected to the Chinese Academy of Sciences in 2009, the World Academy of Sciences (TWAS) in 2020, and the American Institute for Medical and Biological Engineering (AIMBE) in 2026. In 2021, he joined the Chinese University of Hong Kong, Shenzhen, as Dean of School of Science and Engineering and X. Q. Deng Presidential Chair Professor. Since 2026, he has been serving as Vice President of CUHK-Shenzhen. He is now serving as Editor-in-Chief of Aggregate.

2. The origin of low quantum yields of NIR-II small molecules

The fluorescence quantum yield (Φ_{PL}) was defined as the ratio of the number of fluorescent photons emitted by a fluorescent substance to the number of absorbed excitation light photons, which was used to determine the luminous efficiency of fluorophores. Due to the inclusion of both radiative and non-radiative transitions in the decay process of excited-state molecules, Φ_{PL} could be also expressed as

$$\Phi_{PL} = \frac{K_r}{K_r + K_{nr}}$$

K_r is the radiative decay rate and K_{nr} is the non-radiative decay rate.

According to the wave functions reported by Siebrand and Weng *et al.*,[26,27] K_r and K_{nr} could be simplified to

$$K_r \propto \frac{4|J|^2}{3\hbar^4 c^3}(\Delta E)^3$$

$$K_{nr} \propto \alpha \exp(-\beta \Delta E)$$

where J is the electronic transition dipole moment matrix element under the Condon approximation; α is the parameter which represents the electronic coupling part; and β is the decay factor, which is relative to the molecular vibrational coupling strength S ($\beta \propto \ln S^{-1}$).

As the emission wavelength (λ) increases, the corresponding energy gap ($\Delta E = hc/\lambda$) narrows. According to the above equations, K_r decreases sharply with decreasing ΔE, whereas K_{nr} rises exponentially as ΔE diminishes. Furthermore, organic molecules typically exhibit larger vibrational coupling constants (*i.e.*, smaller β values) compared to the inorganic nanomaterials, primarily due to the high-frequency vibrations of C–H bonds,[28] which further elevate K_{nr}. Consequently, the

photoluminescence Φ_{PL} decreases markedly with increasing emission wavelength, particularly in the NIR-II region, a trend fundamentally explained by the energy gap law. Extending this framework, Caram *et al.* developed the energy gap law quantum yield master equation (EQME) to quantitatively describe these effects and predicted a consistent upper limit for achievable quantum yields in the NIR-II window, which indicated the precipitous falloff of QY around 900 nm and the QY beyond 1200 nm is extremely low (Fig. 1).[25]

It should be noted that K_r and K_{nr} were not isolated, and they have shown inherent interactions. In 1981, Siebrand *et al.* proposed the electronic transition propensity rule to illustrate the inherent interactions between K_r and K_{nr}.[26] This rule states that, for a series of structurally similar molecules or the same molecule under comparable external conditions (the molecules have weak electron–phonon coupling and larger β, especially for structurally symmetrical and rigid dyes), when the radiative decay rate increases, the competing non-radiative decay rate increases correspondingly. In other words, for a given molecular electronic state, the contribution of the electronic coupling matrix elements to the radiation and non-radiation rate constants maintains a fixed proportion. Therefore, suppressing the vibrational coupling contribution to non-radiative decay seems to be the sole method to enhance the fluorescence quantum yields. Notably, even though the electronic transition propensity rule is not universally applicable to all NIR-II molecules owing to their large electron–phonon coupling and strong intramolecular D–A strength, it still provides indicative significance, and thereby suppressing the intramolecular vibrational coupling is crucial for improving NIR-II QY.

On the other hand, for common NIR-II small molecules in the isolated state, suppressing the vibrational coupling is actually an effective method to elevate the QYs at the molecular level. Owing to the conjugated structures and the existence of multiple aromatic rings, NIR-II small molecules generally display poor solubility in water or PBS, which leads to the aggregation of NIR-II fluorophores in these media. Even some water-soluble groups such as zwitterions and PEG could be decorated into the fluorophores, the resulted NIR-II compounds prefer to assemble into nanoparticles (such as micelles and vesicles) in water,[29] originating from the extremely hydrophobic properties of fluorophore cores. Therefore, the aggregation of the NIR-II fluorophores seems inevitable under current circumstances. Compared to the fluorescence quantum yields in the dispersed state, the aggregated fluorescence quantum yields are more important parameters for biomedical applications. Thus, in addition to the intramolecular vibrational coupling, the intermolecular excitonic coupling also plays a vital part in the fluorescence quantum yields of NIR-II aggregates.[30–32] Moreover, in the aggregated state, the electronic coupling part is also nonnegligible, which directly determines K_r.[33] In a word, aggregate science may offer a new perspective for mitigating the energy gap law effect on the quantum yield in the NIR-II window. The following are some examples which attempt to boost NIR-II QYs at the molecular and aggregate levels.

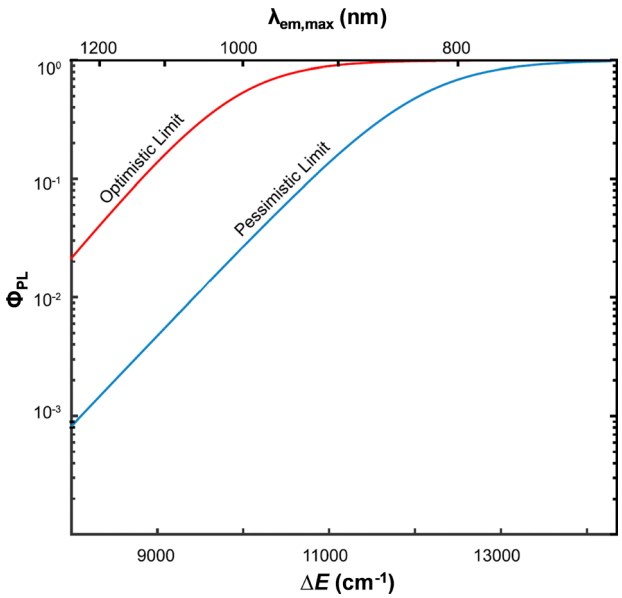

Fig. 1 The predicted consistent upper bounds for NIR-II QY by Caram *et al.*[25]

3. Possible strategies

3.1. Boosting QY at the molecular level (suppressing the intramolecular vibrational coupling)

3.1.1. Deuteration. NIR-II organic molecules usually contain a large amount of C–H/N–H bonds with the fundamental frequency vibration energy of about 3000 cm^{-1}. When the emission reaches the NIR-II region, the electronic energy gap for 1000 nm and 1100 nm photons is 10 000 cm^{-1} and 9091 cm^{-1}, respectively, which is very close to the energy of second overtone (n = 3) of high-frequency C–H/N–H vibrations. The above situation endows the ease of consuming the excited state energy by coupling multiple high-frequency vibrations, which significantly accelerates non-radiative decay. Compared to C–H/N–H bonds, C–D (deuterium) bonds show markedly decreased vibration energy (2100 cm^{-1}) resulting from the larger atomic number of deuterium, thus leading to the decreased K_{nr}. In 2024, Tang and Zhao *et al.* reported a deuterated NIR-II molecule NDA-PDTPE with enhanced QY (Fig. 2a).[34] Through replacing the ten hydrogens in tetraphenylethylene (TPE) rotors with deuterium, NDA-PDTPE with 20 deuterium atoms was prepared and exhibited a lower K_{nr} (5.4×10^8 s^{-1}) compared to the non-deuterated molecule NDA-PTPE (5.8×10^8 s^{-1}) and the QY of NDA-PDTPE was hence improved from 5.94% to 6.23% in toluene. Notably, the fabricated NDA-PDTPE nanoparticles (NPs) exhibited an emission maximum at 1000 nm and a higher QY than NDA-PTPE NPs. The large emission redshift of NDA-PDTPE NPs compared to NDA-PDTPE in toluene solution was probably due to the strong π–π interactions between central naphthalimide acceptors.[35] Even though the QY increased only slightly, probably due to the existence of a large number of

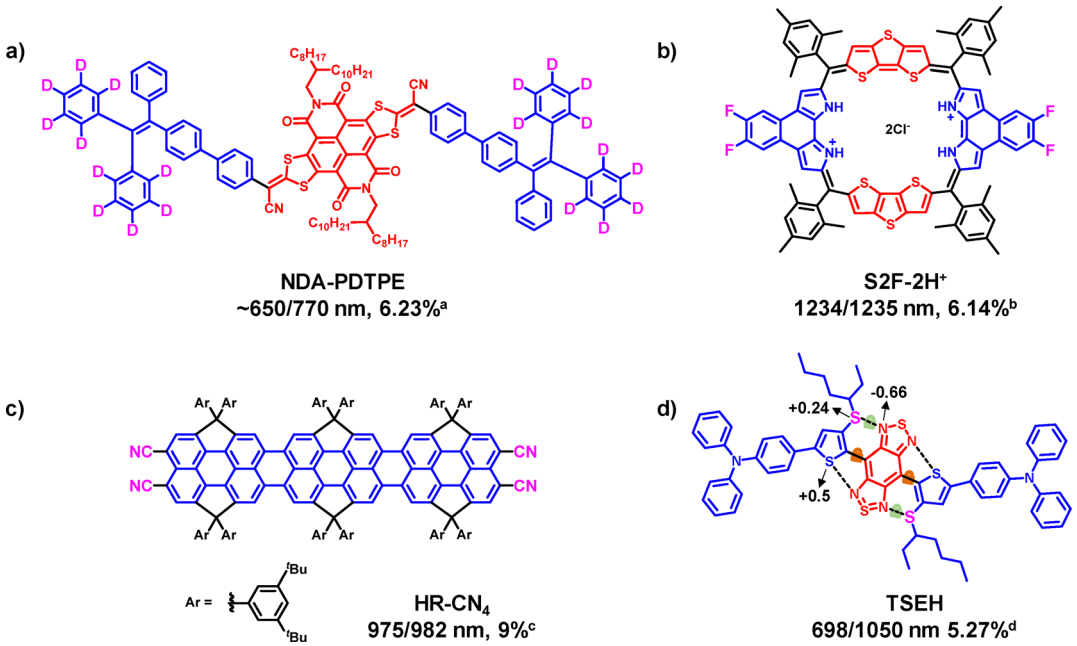

Fig. 2 The chemical structures of typical NIR-II molecules with high QY at the molecular level, and the absorption/emission and QYs of these molecules. (a) Relative QY in toluene using ICG (13%) as a reference; (b) relative QY in CH_2Cl_2 using IR-1061 (0.59%) as a reference; (c) absolute QY in CH_2Cl_2; (d) absolute QY in toluene.

non-deuterated atoms, this research affords us a general strategy to improve QY in the NIR-II window.

3.1.2. Annulation. According to the Marcus theory,[36] the vibration-coupled mediated internal conversion process, governed from high-frequency C–H vibrations,[37] was highly dependent on reorganization energy. As reorganization energy decreased, the internal conversion rates decrease rapidly. Therefore, decreasing the reorganization energy may be a feasible method to improve NIR-II QY. In 2025, Chan, Hsu and Huang *et al.* synthesized a series of 34 π-electron annulated porphyrinoids with pseudo-2D molecular frameworks.[38] All the molecules show emission maximum at >1200 nm with a very small Stokes shift (<11 nm). Notably, the annulated structures of the four molecules, including S2F-2H$^+$, increase the π electron delocalization and structural rigidity,[39] leading to minor structural changes in the transition, including the bond length and bond angle change and conformation change of the whole molecules. The smaller structural changes of the four molecules were responsible for their smaller reorganization energy, compared to the 1D linear analogues. Therefore, all four molecules displayed high QY (>1%) in CH_2Cl_2, which was much higher than that of the previously reported NIR-II molecules with emission beyond 1200 nm. The molecule S2F-2H$^+$ with the minimum reorganization energy (10.5 meV) exhibited the highest QY of 6.14% (Fig. 2b), which showed bright imaging of vasculature structures. This work provides a novel paradigm for achieving ultrabright NIR-II fluorophores through annulation, particularly in the wavelength region beyond 1200 nm.

3.1.3. Rigidification. In addition to the high-frequency C–H/N–H vibrations, the motion of the molecular backbone in the excited state, particularly the fluorophores with flexible backbones, could also consume plenty of excited energy for generating heat, which remarkably contributes to non-radiative decay. Thus, the fluorophores with large and rigid backbones may weaken the excited state molecular motion and principally improve NIR-II QY at the molecular level. However, the rigid molecules with large π conjugation usually face the severe drawbacks of aggregation-caused quenching (ACQ) effect, which needs overall consideration. In 2025, Wu *et al.* reported a series of CN-terminated dicyclopentadiene-fused rylenes.[40] When three perylene units were embedded (Fig. 2c), the molecule was denoted as HR-CN_4 and its absorption/emission maximum was centered at 975/982 nm. The rigid rylene backbone not only endows HR-CN_4 with large molar absorption coefficient (8×10^4 M^{-1} cm^{-1}), but also decreases the excited state molecular motion, causing the ultrahigh absolute QY of 9% in CH_2Cl_2. Notably, the bulky *tert*-butyl benzene groups attached to the cyclopentadiene rings, formatted by sp^3 carbon atom fusion at bay positions of perylene units, block the intermolecular aggregation of large π rylenes and are beneficial to the bright emission in solution. On the other hand, the electron-withdrawing CN groups increase the molecular donor–acceptor strength and improve its stability. In addition, dipole–dipole interactions between CN groups and pericarbons facilitate the formation of one-dimensional linear assembly (most like J aggregates), which was also accountable for its high QY. In a word, this study inspires the employment of rigid backbones for NIR-II fluorophores with high brightness.

3.1.4. Noncovalent locking. Although employing fused ring systems as the backbone is an effective method to enhance molecular rigidity, it typically requires complex synthetic procedures. Intramolecular noncovalent interactions provide

another way to address the above issue. Through the introduction of intramolecular electrostatic locking by alkylthio side chains, an improved QY of the TSEH molecule, compared to its analogue TEH with alky side chains, was realized by Tang *et al.* in 2024.[41] As shown in Fig. 2d, the carbon atoms on the alkyl side chains of the thiophene bridge were replaced with sulfur atoms in TSEH. Owing to the larger atom radius and low electronegativity of sulfur (electronegativity: S, 2.58; C, 2.55; O, 3.44), the sulphur atoms on the side chain of the thiophene bridge unit show positive charge (+0.24*e*) and the nitrogen atoms on the benzobisthiadiazole (BBTD) unit show negative charge (−0.66*e*). Thus, two electrostatic locks between the thiophene bridge and BBTD units were formed. Combining with the other two electrostatic locks from the sulphur atoms on thiophene rings (+0.5*e*) and nitrogen atoms on BBTD unit (−0.66*e*), the molecular motion (including rotation of C–C bond and intramolecular vibrations) of the conjugated backbone was significantly suppressed, leading to reduced non-radiative decay. Owing to the dominance of internal conversion rate (k_{ic}) in non-radiative decay rate of NIR-II molecules, the k_{ic} of TEH and TSEH were also calculated. The results indicated that TSEH (5.56×10^8 s^{-1}) displayed a value one order of magnitude lower than that of TEH (4.67×10^9 s^{-1}) through inhibiting the distortion of central BBTD units, which is consistent with the higher QY of TSEH compared to TEH. Notably, the enhanced backbone rigidity not only gives TSEH high QY, but also affords increased molar absorption coefficient due to the smaller skeleton distortion (1.67×10^4 and 1.30×10^4 M^{-1} cm^{-1} for TSEH and TEH, respectively). Consequently, TSEH displays an absolute QY of 5.27% in toluene and relative QY of 1.22% in NPs, which was much higher than TEH in their counterparts.

3.2. Boosting QY at the aggregate level (tuning the intermolecular excitonic coupling)

3.2.1. Long terminal alkyl chains. When two or more chromophores are brought into close proximity in space, interactions occur between their electron clouds. The exciton (electron–hole pair) generated upon excitation of one molecule is no longer confined to that single molecule but can delocalize onto adjacent molecules, which is called exciton coupling. For NIR-II molecules with coplanar conformation and large π conjugation, the fluorophores may aggregate severely in water or in the solid state. The intensive intermolecular excitonic coupling in the aggregated state, such as H aggregates, could promote non-radiative decay and cause serious decline of QY.[31] Therefore, increasing the spatial isolation of fluorophores to decrease their intermolecular interactions may be a feasible method to reduce the detrimental intermolecular excitonic coupling.

In 2025, Tang, Wang and Zhang *et al.* reported a high-luminance NIR-II molecule AOTTIT with aggregation-induced emission (AIE) properties (Fig. 3a).[42] AOTTIT employs strong electron-deficient *s*-indacene-1,3,5,7(2*H*,6*H*)-tetraone as electron acceptors and thiophene-substituted triphenylamine as electron donors, and the peripheral triphenylamine units were decorated with four long branched alkyl chains. Notably, the long terminal alkyl chains were beneficial for the spatial

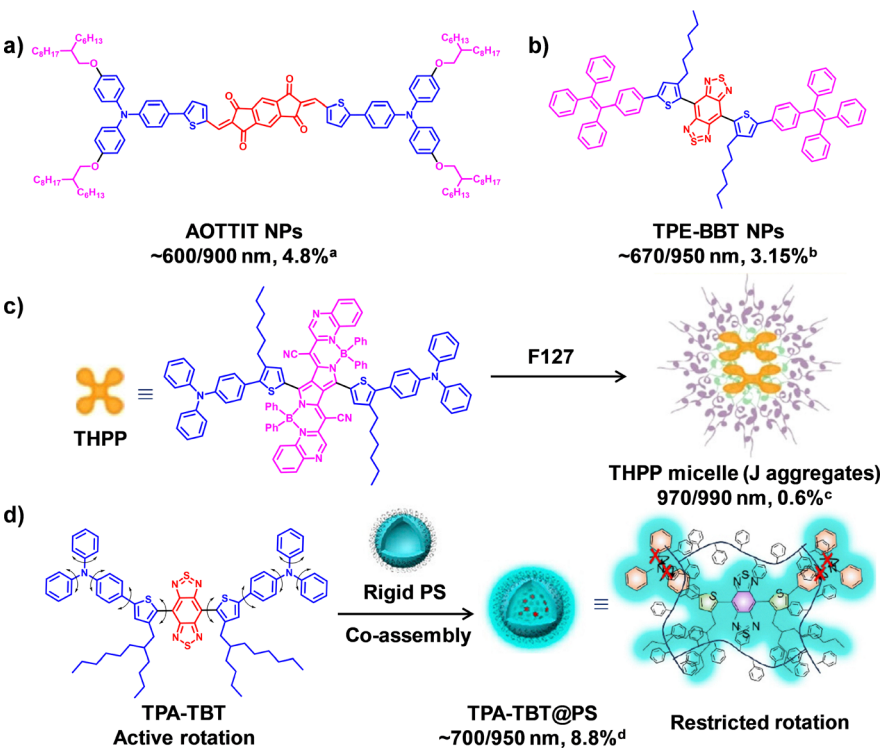

Fig. 3 A schematic representation of boosted QY at the aggregate level. (a) Absolute QY in NPs; (b) relative QY in NPs using IR26 (0.05%) as a reference; (c) relative QY in NPs using IR26 (0.05%) as a reference; (d) absolute QY in NPs. Reproduced from ref. 45 and 46 with permission from Wiley-VCH and American Chemical Society, respectively.

isolation of the central coplanar fluorophores and weakening the intermolecular excitonic coupling. Therefore, AOTTIT NPs displayed a main absorption/emission peak at about 600/900 nm with a high absolute QY of 4.8%, which was much higher than that of its analogue TTIT without alkyl chains. It should be noted that, even though TTIT shows a relatively high QY (2.8%) in THF solution, its emission was seriously quenched in the aggregated state (ACQ molecule), further suggesting the importance of long alkyl chains in improving the aggregated QY. This research affords us some new thoughts for designing high-luminance NIR-II molecules by alkyl chain engineering.

3.2.2. Introduction of TPE rotors. For ''D–A–D'' type NIR-II molecules, the twisted intramolecular charge transfer (TICT) effect was nonnegligible for their low QY in aqueous solution. TICT is an electron transfer process in ''D–A'' molecules linked by a single bond. Upon photoexcitation, the molecules undergo intramolecular rotation, which twists their conformation and diminishes orbital overlap. In nonpolar solvents, the molecules adopt a coplanar conformation with a sharp emission spectrum. In polar solvents, particularly water, the TICT state forms and the molecules show broad and shifted emission with weakened intensity, originating from the varying twist angles of individual luminogens, elevated HOMO levels and the susceptibility of the TICT state to various nonradiative quenching processes. Typically, in NIR-II molecules, BBTD was employed as the electron acceptor and triphenylamine, thiophene and dioxy thiophene were used as the electron donors. When excited in a polar solvent such as water, the electron acceptor and donor of NIR-II molecules will rotate around the single bond and a new TICT state with lower energy was formed to stabilize its large dipole moment, leading to the decreased QY and increased non-radiative decay. In general, the stronger D–A interaction will contribute to an enhanced TICT effect. Therefore, fine-tuning the molecular D-A interaction was important for improving QY. In 2022, Tang and Zhang *et al.* reported an ultrabright NIR-II AIEgen TPE-BBT by employing TPE groups as electron donors (Fig. 3b).[43] The decoration of TPE on the fluorophore skeleton shows some important roles: (1) TPE displayed weaker electron donating ability compared to triphenylamine, which was beneficial for mitigation of the TICT effect. (2) Stronger intermolecular interactions were observed in the crystals of TPA-BBT compared to its analogue TPA-BBT with triphenylamine as electron donors, leading to the enhanced restriction of intramolecular motion (RIM) effect; (3) in addition, the noncovalent interactions between TPE and aromatic rings could affect the orientation of the fluorophore, thus reducing the detrimental intermolecular excitonic coupling. Consequently, TPE-BBT crystals exhibited the highest absolute QY of 10.4% so far, and a quite high absolute QY of 1.8% in water was also observed for TPE-BBT NPs. The ultrahigh QY of TPE-BBT enhances its performance in NIR-II photoluminescence and chemiluminescence bioimaging, which brings new possibilities for constructing bright NIR-II molecules through introduction of TPE rotors.

3.2.3. J-aggregates. J-aggregation is another important aggregation mode with intensive intermolecular excitonic coupling. The dyes in J aggregates were aligned in head to tail with a decreased excited energy. The above feature endows J-aggregates with an enlarged molar extinction coefficient, extended absorption and emission wavelength and improved QY. Thus, the induction of formation of J aggregates is a credible method to mitigate the energy gap law effect on NIR-II QY, and many dyes such as BODIPY, naphthalene diimide and cyanine derivatives were employed to fabricate NIR-II aggregates.[44] In 2021, Zhang and Fan developed a dibodipy-based NIR-II molecule THPP with typical J-aggregation characteristic (Fig. 3c).[45] The absorption/emission of THPP in THF was located at 900/932nm with a molar extinction coefficient (ε) of 2.0×10^5 M^{-1} cm^{-1} and a QY of 0.07%. Notably, the whole planar conformation of THPP was favorable for ordered packing in the aggregated state. When dispersed in a mixture of THF/H_2O = 1 : 9, the absorption/emission of THPP redshifted to 980/1006 nm, the molar extinction coefficient increased to 2.2×10^5 M^{-1} cm^{-1}, and the QY dramatically raised to $>3.5\%$, strongly supporting the formation of J aggregates. The absolute brightness ($\varepsilon \times \Phi_{PL}$) was determined to be >7700 in THF/H_2O = 1 : 9, which was extremely high for NIR-II fluorophores. Furthermore, THPP was encapsulated in amphiphilic carriers F127 (PEO_{100}-PPO_{65}-PEO_{100}) to form micelles. The absorption/emission of the THPP micelle was centered at 970/990 nm with ε of 2.4×10^5 M^{-1} cm^{-1} and QY of 0.6%, further demonstrating J aggregate formation in micelles. The absolute brightness of the THPP micelle was 1440, which was still a rather high value. In brief, this research inspires us to design the NIR-II probe with both a large molar extinction coefficient and a high QY by J-aggregates.

3.2.4. Rigid polymer carriers. Owing to the large hydrophobicity, NIR-II molecules were generally entrapped in carriers to improve their water solubility and stability. Hence, the carriers, such as amphiphilic polymers, have a significant influence on QY of the resulted nanoprobes. In 2024, an ultrabright nanoprobe TPA-TBT@PS was reported by Hu and Tian *et al.* by using the rigid polystyrene (PS) as carriers (Fig. 3d).[46] The rigid polymer backbone of PS almost completely suppressed the molecular motion of TPA-TBT, thus reducing the non-radiative decay. In addition, the existence of many aromatic rings in PS may also induce partial spatial isolation of fluorophores, causing the decreased intermolecular excitonic coupling. On the other hand, a powerful hydrophobic core could be formed due to the highly hydrophobicity of PS, which was beneficial for shielding water molecules and thereby mitigating the TICT effect, particularly for TPA-TBT with a typical twisted D–A–D structure. The above features give rise to the high absolute QY of 8.82% for TPA-TBT@PS in water, which was two times that of its counterpart with DSPE as carrier (4.25%). Apart from PS, the polymer with a similar rigid backbone, such as poly(α-methyl styrene), and some water-soluble supramolecular macrocycles with typical cavities and rigid structures (such as pillararene and cucurbituril) might also be used as carriers for elevating the QY of NIR-II molecules. In a word, this work presents a novel avenue to maximize the QY of the nanoprobe by optimizing the polymer carriers.

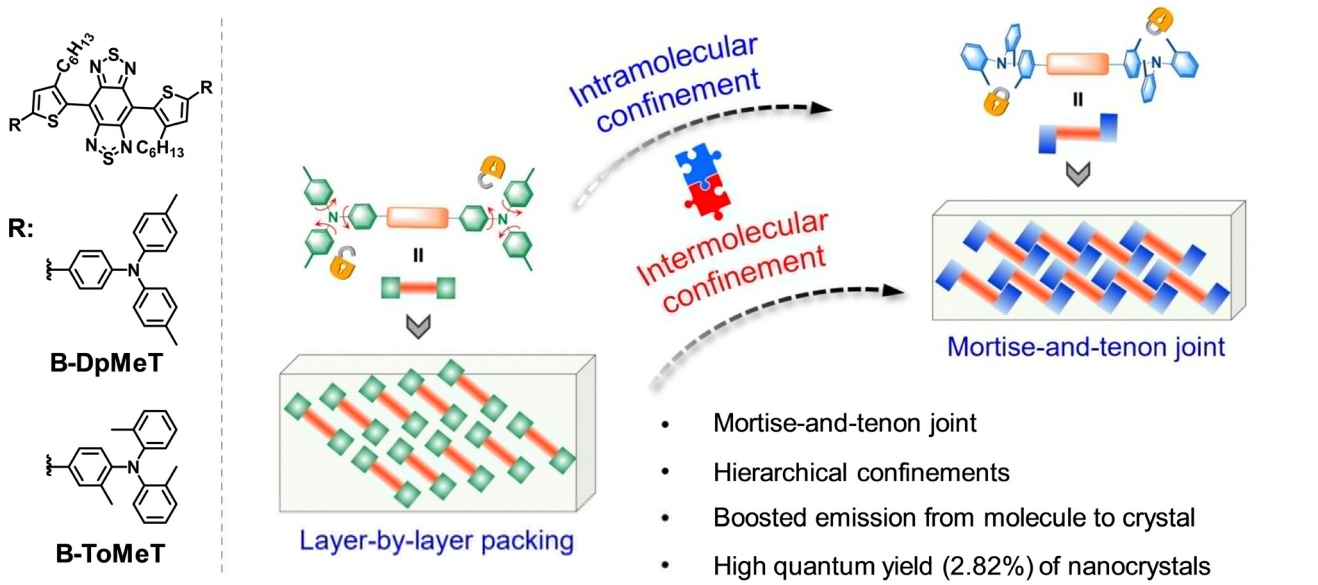

Fig. 4 A schematic representation of simultaneously boosted QY at the molecular and aggregate level from rational molecular design. Reproduced from ref. 47 with permission from American Chemical Society.

3.3. Synergistic effect

Notably, the QY at the molecular and aggregate level could be simultaneously improved by a single strategy, leading to a synergistic effect. In 2025, Zhao *et al.* reported a high-brightness NIR-II nanoprobe *via* hierarchical confinements.[47] Through methyl substitution at the *ortho*-position of benzene rings in triphenylamine, B-ToMeT was obtained (Fig. 4). Notably, methyl substitution not only restricts the free rotation of triphenylamine, leading to suppressed intramolecular vibrational coupling, but also could regulate the packing mode to form a mortise-and-tenon joint in aggregates, which results in further enhanced rigidity of the molecular surroundings (RIM effect) and reduced detrimental intermolecular excitonic coupling. In addition, B-ToMeT nanocrystals were readily formulated using microfluidics technology due to their distinctive packing arrangement. The above features afford B-ToMeT both higher QY in THF solution (0.393%), nanocrystals (2.82%) and crystals (9.7%) than its counterpart B-DpMeT without methyl substitution (0.066%, 1.02% and 4.3% in THF, NPs and crystals, respectively), which inspires us to design high-luminescence efficiency NIR-II materials through synergistic intramolecular and intermolecular effects.

4. Conclusions

Significant progress has been made in the development of NIR-II-emissive small molecules, which continue to attract considerable research interest in chemistry and materials science. The successful preparation and application of these molecules have substantially advanced *in vivo* bioimaging and demonstrate promising potential for clinical translation. However, the intrinsically low fluorescence QYs of NIR-II molecules, governed by the energy gap law, can compromise imaging performance and ultimately hamper their practical applications. Therefore, circumventing the limitations imposed by the energy gap law to construct ultrabright NIR-II nanoprobes (typically with QY $>5\%$) remains a crucial and persistent challenge.

In recent years, several innovative strategies have been proposed to enhance NIR-II QY at both the molecular and aggregate levels. On the molecular level, where vibrational coupling dominates non-radiative decay, approaches such as deuteration, annulation, rigidification and noncovalent locking have been employed to suppress intramolecular vibrational coupling and thereby improve the intrinsic molecular QY. On the aggregate level, modulation of intermolecular excitonic coupling, through suppression of detrimental interactions (*e.g.*, *via* long alkyl chain engineering) or promotion of favorable packing (*e.g.*, J-aggregation), can effectively enhance emission in the solid or aggregated state. Notably, integrated molecular design strategies that simultaneously boost molecular and aggregate QYs offer a promising direction for future material development. Despite the considerable achievements, NIR-II molecules exhibiting QYs exceeding 5% remain scarce, particularly in aggregated forms.

Moving forward, several key considerations should guide the design of high-brightness NIR-II materials. First, suppressing high-frequency C–H/N–H vibrations remains essential. Strategies such as deuteration and fluorination can enhance QY without significantly altering absorption/emission. Fluorination is particularly noteworthy, as it not only reduces vibrational energy loss (C–F vibration $\approx$ 1100 cm^{-1}) but also diminishes aqueous quenching by weakening interactions with water molecules.

Second, molecular packing should be tailored through rational molecular design and aggregation state regulation. Ordered arrangements such as J-aggregates and interlocked ''mortise-and-tenon'' architectures can restrict molecular

motion and reduce detrimental exciton coupling. What's more, a holistic design approach is necessary to concurrently optimize both molecular and aggregated QYs. For example, under some circumstances, the planar backbones for higher QYs at the molecular level may lead to detrimental intermolecular stacking, thus reducing the aggregated QYs. Therefore, the molecular structure design and aggregation state regulation are complementary and the antagonistic effects should be avoided.[48] Furthermore, since the brightness of fluorophores are defined as the product of molar absorption coefficient and quantum yield, improving the molar absorption coefficients of NIR-II molecules are also crucial for higher brightness.[49–51] Such efforts will require meticulous molecular engineering and systematic optimization. In summary, continued innovation in molecular design and aggregation control is crucial to overcoming the low QY bottleneck in NIR-II small molecules. Advances in this direction will accelerate the translation of NIR-II fluorescence imaging into broader biomedical and clinical practice.

Author contributions

Yi Qin, Dong Wang and Ben Zhong Tang put forward the idea. Yi Qin collected the literature and wrote the original draft. Dong Wang and Ben Zhong Tang reviewed and edited the manuscript.

Conflicts of interest

The authors declare no competing financial interest.

Data availability

No primary research results, software or code have been included and no new data were generated or analysed as part of this review.

Acknowledgements

The authors are grateful for the financial support from the National Key Research and Development Program of China (2024YFA1212100), the National Natural Science Foundation of China (22575154 and 52573204), the Guangdong Basic and Applied Basic Research Fund (Guangdong Natural Science Fund) (2025A1515012174), and the Science and Technology Foundation of Shenzhen City (JCYJ20241202124423032). The authors also acknowledge the Scientific Foundation for Youth Scholars of Shenzhen University.

References

1 E. Betzig, G. H. Patterson, R. Sougrat, O. W. Lindwasser, S. Olenych, J. S. Bonifacino, M. W. Davidson, J. Lippincott-Schwartz and H. F. Hess, Imaging Intracellular Fluorescent Proteins at Nanometer Resolution, *Science*, 2006, **313**, 1642–1645.

2 A. L. Vahrmeijer, M. Hutteman, J. R. van der Vorst, C. J. H. van de Velde and J. V. Frangioni, Image-guided cancer surgery using near-infrared fluorescence, *Nat. Rev. Clin. Oncol.*, 2013, **10**, 507–518.

3 R. Blau, O. Shelef, D. Shabat and R. Satchi-Fainaro, Chemiluminescent probes in cancer biology, *Nat. Rev. Bioeng.*, 2023, **1**, 648–664.

4 D. Yan, D. Wang and B. Z. Tang, In vivo, clinical and translational aspects of aggregation-induced emission, *Nat. Rev. Bioeng.*, 2025, **3**, 976–991.

5 E. L. Schmidt, Z. Ou, E. Ximendes, H. Cui, C. H. C. Keck, D. Jaque and G. Hong, Near-infrared II fluorescence imaging, *Nat. Rev. Methods Primers*, 2024, **4**, 23.

6 Y. Yang, Y. Chen, P. Pei, Y. Fan, S. Wang, H. Zhang, D. Zhao, B.-Z. Qian and F. Zhang, Fluorescence-amplified nanocrystals in the second near-infrared window for in vivo real-time dynamic multiplexed imaging, *Nat. Nanotechnol.*, 2023, **18**, 1195–1204.

7 Z. Chen, I. Gezginer, Q. Zhou, L. Tang, X. L. Deán-Ben and D. Razansky, Multimodal optoacoustic imaging: methods and contrast materials, *Chem. Soc. Rev.*, 2024, **53**, 6068–6099.

8 L. He, Y. Li, C. Zhang, X. Zhang, B. Wang, T. Ren and L. Yuan, Development of small-molecule NIR-II photothermal agents for image-guided tumor therapy, *Coord. Chem. Rev.*, 2025, **533**, 216549.

9 Y. Liu, Y. Li, S. Koo, Y. Sun, Y. Liu, X. Liu, Y. Pan, Z. Zhang, M. Du, S. Lu, X. Qiao, J. Gao, X. Wang, Z. Deng, X. Meng, Y. Xiao, J. S. Kim and X. Hong, Versatile Types of Inorganic/Organic NIR-IIa/IIb Fluorophores: From Strategic Design toward Molecular Imaging and Theranostics, *Chem. Rev.*, 2022, **122**, 209–268.

10 D. Yan, Z. Li, M. M. S. Lee, B. Z. Tang and D. Wang, NIR-II AIEgens for Infectious Diseases Phototheranostics, *Angew. Chem., Int. Ed.*, 2024, **63**, e202414259.

11 D. Ma, H. Bian, M. Gu, L. Wang, X. Chen and X. Peng, Recent advances in the design and applications of near-infrared II responsive small molecule phototherapeutic agents, *Coord. Chem. Rev.*, 2024, **505**, 215677.

12 Z. Lei and F. Zhang, Molecular Engineering of NIR-II Fluorophores for Improved Biomedical Detection, *Angew. Chem., Int. Ed.*, 2021, **60**, 16294–16308.

13 J. Mu, M. Xiao, Y. Shi, X. Geng, H. Li, Y. Yin and X. Chen, The Chemistry of Organic Contrast Agents in the NIR-II Window, *Angew. Chem., Int. Ed.*, 2022, **61**, e202114722.

14 Y. Fang, J. Shang, D. Liu, W. Shi, X. Li and H. Ma, Design, Synthesis, and Application of a Small Molecular NIR-II Fluorophore With Maximal Emission Beyond 1200 nm, *J. Am. Chem. Soc.*, 2020, **142**, 15271–15275.

15 A. L. Antaris, H. Chen, K. Cheng, Y. Sun, G. Hong, C. Qu, S. Diao, Z. Deng, X. Hu, B. Zhang, X. Zhang, O. K. Yaghi, Z. R. Alamparambil, X. Hong, Z. Cheng and H. Dai, A Small-Molecule Dye for NIR-II Imaging, *Nat. Mater.*, 2016, **15**, 235–242.

16 L. Xu, Q. Zhang, X. Wang and W. Lin, Biomedical applications of NIR-II organic small molecule fluorescent probes in different organs, *Coord. Chem. Rev.*, 2024, **519**, 216122.
17 Z. Hu, L. Feng and P. Yang, *Adv. Funct. Mater.*, 2024, **34**, 2310818.
18 C. Sun, B. Li, M. Zhao, S. Wang, Z. Lei, L. Lu, H. Zhang, L. Feng, C. Dou, D. Yin, H. Xu, Y. Cheng and F. Zhang, J-Aggregates of Cyanine Dye for NIR-II in Vivo Dynamic Vascular Imaging beyond 1500 nm, *J. Am. Chem. Soc.*, 2019, **141**(49), 19221–19225.
19 W. E. Meador, E. Y. Lin, I. Lim, H. C. Friedman, D. Ndaleh, A. K. Shaik, N. I. Hammer, B. Yang, J. R. Caram, E. M. Sletten and J. H. Delcamp, Silicon-RosIndolizine fluorophores with shortwave infrared absorption and emission profiles enable in vivo fluorescence imaging, *Nat. Chem.*, 2024, **16**, 970–978.
20 R. Wei, Y. Dong, X. Wang, J. Li, Z. Lei, Z. Hu, J. Chen, H. Sun, H. Chen, X. Luo, X. Qian and Y. Yang, Rigid and Photostable Shortwave Infrared Dye Absorbing/Emitting beyond 1200 nm for High-Contrast Multiplexed Imaging, *J. Am. Chem. Soc.*, 2023, **145**, 12013–12022.
21 D. Yan, W. Xie, J. Zhang, L. Wang, D. Wang and B. Z. Tang, Donor/π-Bridge Manipulation for Constructing a Stable NIR-II Aggregation-Induced Emission Luminogen with Balanced Phototheranostic Performance, *Angew. Chem., Int. Ed.*, 2021, **60**, 26769–26776.
22 A. Ji, H. Lou, C. Qu, W. Lu, Y. Hao, J. Li, Y. Wu, T. Chang, H. Chen and Z. Cheng, Acceptor engineering for NIR-II dyes with high photochemical and biomedical performance, *Nat. Commun.*, 2022, **13**, 3815.
23 R. Englman and J. Jortner, The energy gap law for radiationless transitions in large molecules, *Mol. Phys.*, 1970, **18**, 145–164.
24 S. J. Jang, A simple generalization of the energy gap law for nonradiative processes, *J. Chem. Phys.*, 2021, **155**, 164106.
25 H. C. Friedman, E. D. Cosco, T. L. Atallah, S. Jia, E. M. Sletten and J. R. Caram, Establishing design principles for emissive organic SWIR chromophores from energy gap laws, *Chem*, 2021, **7**, 3359–3376.
26 G. Orlandi and W. Siebrand, Electronic propensity rule for radiationless transitions, *Chem. Phys. Lett.*, 1981, **80**, 399–403.
27 Y. Zhang, H. Liu and Y. Weng, Theoretical and Experimental Investigation of the Electronic Propensity Rule: A Linear Relationship between Radiative and Nonradiative Decay Rates of Molecules, *J. Phys. Chem. Lett.*, 2023, **14**, 4151–4157.
28 S.-F. Wang, B.-K. Su, X.-Q. Wang, Y.-C. Wei, K.-H. Kuo, C.-H. Wang, S.-H. Liu, L.-S. Liao, W.-Y. Hung, L.-W. Fu, W.-T. Chuang, M. Qin, X. Lu, C. You, Y. Chi and P.-T. Chou, Polyatomic molecules with emission quantum yields >20% enable efficient organic light-emitting diodes in the NIR(II) window, *Nat. Photonics*, 2022, **16**, 843–850.
29 D. Yan, T. Li, Y. Yang, N. Niu, D. Wang, J. Ge, L. Wang, R. Zhang, D. Wang and B. Z. Tang, A Water-soluble AIEgen for Noninvasive Diagnosis of Kidney Fibrosis via SWIR Fluorescence and Photoacoustic Imaging, *Adv. Mater.*, 2022, **34**, e2206643.
30 Q. Peng and Z. Shuai, Molecular mechanism of aggregation-induced emission, *Aggregate*, 2021, **2**, e91.
31 Y. Wang, J. Ren and Z. Shuai, Minimizing non-radiative decay in molecular aggregates through control of excitonic coupling, *Nat. Commun.*, 2023, **14**, 5056.
32 G. D. Scholes, G. R. Fleming, A. Olaya-Castro and R. van Grondelle, Lessons from nature about solar light harvesting, *Nat. Chem.*, 2011, **3**, 763–774.
33 J. Xu, J. Xue, Y. Dai, J. Zhang, J. Ren, C. Yao, S. Li, Q. Meng, X. Wen, H. Shao and J. Qiao, π-Bridge mediated coupling between inter- and intra-molecular charge transfer in aggregates for highly efficient near-infrared emission, *Aggregate*, 2024, **5**, e634.
34 F. Ma, Q. Jia, Z. Deng, B. Wang, S. Zhang, J. Jiang, G. Xing, Z. Wang, Z. Qiu, Z. Zhao and B. Z. Tang, Boosting Luminescence Efficiency of Near-Infrared-II Aggregation-Induced Emission Luminogens via a Mash-Up Strategy of π-Extension and Deuteration for Dual-Model Image-Guided Surgery, *ACS Nano*, 2024, **18**, 9431–9442.
35 S. Cui, S. Fan, H. Tan, Y. Lu, Y. Zha, B. Xu, Y. Liu and D. Cui, Ultra-homogeneous NIR-II fluorescent selfassembled nanoprobe with AIE properties for photothermal therapy of prostate cancer, *Nanoscale*, 2021, **13**, 15569–15575.
36 R. A. Marcus and N. Sutin, Electron Transfers in Chemistry and Biology, *Biochim. Biophys. Acta*, 1985, **811**, 265–322.
37 P. Ghosh, A. M. Alvertis, R. Chowdhury, P. Murto, A. J. Gillett, S. Dong, A. J. Sneyd, H.-H. Cho, E. W. Evans, B. Monserrat, F. Li, C. Schnedermann, H. Bronstein, R. H. Friend and A. Rao, Decoupling excitons from high-frequency vibrations in organic molecules, *Nature*, 2024, **629**, 355–362.
38 Y.-C. Tsai, Y.-C. Chen, H.-F. Lu, K.-M. Chan, S.-L. Lin, P.-X. Lin, R. Rotomskis, S. Steponkiene, T.-K. Wu, M.-H. Chan, J. A. Ho, Y.-F. Huang, C.-P. Hsu and Y.-H. Chan, Energy Gap Law-Harnessing Design of Highly Second Near-Infrared Emissive 34π-Annulated Porphyrinoids for In Vivo Imaging, *J. Am. Chem. Soc.*, 2025, **147**, 21940–21949.
39 B. C. Paulus, S. L. Adelman, L. L. Jamula and J. K. McCusker, Leveraging excited-state coherence for synthetic control of ultrafast dynamics, *Nature*, 2020, **582**, 214–218.
40 L. Jiao, Y. Zou, W. Fan, Y. Han, Q. Zhou, J. Shao and J. Wu, Aggregation-Free, Highly Soluble CN-Terminated Dicyclopentadiene-Fused Rylenes, *J. Am. Chem. Soc.*, 2025, **147**, 9415–9423.
41 X. Wang, X. Yang, G. Jiang, Z. Hu, T. Liao, G. Wang, X. Zhang, X. He, J. Zhang, J. Zhang, W. Cao, K. Zhang, J. W. Y. Lam, J. Sun, H. Sun, Y. Liang and B. Z. Tang, Unlocking the NIR-II AIEgen for High Brightness through Intramolecular Electrostatic Locking, *Angew. Chem., Int. Ed.*, 2024, **63**, e202404142.
42 X. Li, X. Ou, Z. Yang, M. Kang, W. Xu, D. Li, R. T. K. Kwok, J. W. Y. Lam, Z. Zhang, D. Wang and B. Z. Tang, Win–Win Integration of Genetically Engineered Cellular Nanovesicles with High-Absorbing Multimodal Phototheranostic

Molecules for Boosted Cancer Photo-Immunotherapy, *Adv. Mater.*, 2025, **37**, 2416590.

43 H. Shen, F. Sun, X. Zhu, J. Zhang, X. Ou, J. Zhang, C. Xu, H. H. Y. Sung, I. D. Williams, S. Chen, R. T. K. Kwok, J. W. Y. Lam, J. Sun, F. Zhang and B. Z. Tang, Rational Design of NIR-II AIEgens with Ultrahigh Quantum Yields for Photo- and Chemiluminescence Imaging, Rational Design of NIR-II AIEgens with Ultrahigh Quantum Yields for Photo- and Chemiluminescence Imaging, *J. Am. Chem. Soc.*, 2022, **144**, 15391–15402.

44 J. Xu, X. Zheng, T.-B. Ren, L. Shi, X. Yin, L. Yuan and X.-B. Zhang, Recent advances in near-infrared-II organic J-aggregates for bio-applications, *Coord. Chem. Rev.*, 2025, **528**, 216379.

45 Q. Zhang, P. Yu, Y. Fan, C. Sun, H. He, X. Liu, L. Lu, M. Zhao, H. Zhang and F. Zhang, Bright and Stable NIR-II J-Aggregated AIE Dibodipy-Based Fluorescent Probe for Dynamic In Vivo Bioimaging, *Angew. Chem., Int. Ed.*, 2021, **60**, 3967–3973.

46 H. Xu, L. Yuan, Q. Shi, Y. Tian and F. Hu, Ultrabright NIR-II Nanoprobe for Image-Guided Accurate Resection of Tiny Metastatic Lesions, *Nano Lett.*, 2024, **24**, 1367–1375.

47 F. Ma, R. Zhang, B. Wang, Z. Liang, S. Zhang, J. Jiang, H. Tan, G. Xing, R. T. K. Kwok, J. W. Y. Lam, Z. Zhao and B. Z. Tang, High-Luminescence Efficiency NIR-II Nanocrystals via Hierarchical Confinements for Imaging-Guided Surgery of Acute Intestinal Ischemia, *J. Am. Chem. Soc.*, 2025, **147**(33), 29815–29828.

48 P. Chowdhury, H.-F. Lu, H.-T. Huang, M.-H. Liu, Y.-C. Chen, K.-M. Chan, S.-L. Lin, R. Rotomskis, S. Steponkiene, T.-K. Wu, Y.-F. Huang, C.-P. Hsu and Y.-H. Chan, Asymmetric Xanthene with Noncovalent Conformation Locks to Attain High Fluorescence >1500 nm, *J. Am. Chem. Soc.*, 2026, **148**, 17764–17778.

49 Y. Song, X. Tong, Y. Han and Q.-W. Zhang, Finely tunable NIR-II organic scaffolds forfluorescence/photoacoustic duplex imaging–guided noninvasive photothermal therapy of glioblastoma, *Aggregate*, 2025, **6**, e680.

50 H. Li, Q. Li, Y. Gu, M. Wang, P. Tan, H. Wang, L. Han, Y. Zhu, F. He and L. Tian, Dimerization extends π-conjugation of electron donor-acceptor structures leading to phototheranostic properties beyond the sum of two monomers, *Aggregate*, 2024, **5**, e528.

51 S. Yang, Q. Jia, X. Ou, F. Sun, C. Song, T. Zhao, R. T. K. Kwok, J. Sun, Z. Zhao, J. W. Y. Lam, Z. Wang and B. Zhong Tang, Integration of Motion and Stillness: A Paradigm Shift in Constructing Nearly Planar NIR-II AIEgen with Ultrahigh Molar Absorptivity and Photothermal Effect for Multimodal Phototheranostics, *J. Am. Chem. Soc.*, 2025, **147**, 3570–3583.

